

Functional consequences of altered glycosylation of tumor-associated hypoxia biomarker carbonic anhydrase IX

Magdalena BARATOVA*, Lucia SKVARKOVA*, Maria BARTOSOVA, Lenka JELENSKA, Miriam ZATOVICOVA, Barbora PUZDEROVA, Ivana KAJANOVA, Lucia CSADEROVA*, Silvia PASTOREKOVA, Eliska SVASTOVA

Biomedical Research Center, Institute of Virology, Department of Cancer Biology, Slovak Academy of Sciences, Bratislava, Slovakia

*Correspondence: lucia.csaderova@savba.sk

*Contributed equally to this work.

Received May 5, 2023 / Accepted June 20, 2023

Glycosylation is a posttranslational modification of proteins affecting numerous cellular functions. A growing amount of evidence confirms that aberrant glycosylation is involved in pathophysiological processes, including tumor development and progression. Carbonic anhydrase IX (CAIX) is a transmembrane protein whose expression is strongly induced in hypoxic tumors, which makes it an attractive target for anti-tumor therapy. CAIX facilitates the maintenance of intracellular pH homeostasis through its catalytic activity, which is linked with extracellular pH acidification promoting a more aggressive phenotype of tumor cells. The involvement of CAIX in destabilizing cell-cell contacts and the focal adhesion process also contributes to tumor progression. Previous research shows that CAIX is modified with N-glycans, O-glycans, and glycosaminoglycans (GAG). Still, the impact of glycosylation on CAIX functions has yet to be fully elucidated. By preparing stably transfected cells expressing mutated forms of CAIX, unable to bind glycans at their defined sites, we have attempted to clarify the role of glycan structures in CAIX functions. All three types of prepared mutants exhibited decreased adhesion to collagen. By surface plasmon resonance, we proved direct binding between CAIX and collagen. Cells lacking glycosaminoglycan modification of CAIX also showed reduced migration and invasion, indicating CAIX glycosaminoglycans' involvement in these processes. Analysis of signaling pathways affected by the loss of GAG component from CAIX molecule revealed decreased phosphorylation of c-Jun, of p38 α kinase, focal adhesion kinase, and reduced level of heat shock protein 60 in cells cultured in hypoxia. Cells expressing CAIX without GAG exhibited increased metabolon formation and increased extracellular pH acidification. We also observed reduced CAIX GAG glycans in the inflammatory environment in hypoxia, pathophysiological conditions reflecting *in vivo* tumor microenvironment. Understanding the glycan involvement in the characteristics and functions of possible targets of cancer treatment, such as cell surface localized CAIX, could improve the therapy, as many drugs target glycan parts of a protein.

Key words: glycan; glycosaminoglycan; carbonic anhydrase IX; hypoxia; signaling pathways; inflammation

Cancer progression is associated with a range of alterations in extracellular and intracellular signaling that promote cell proliferation, dissociation of malignant cells from the primary tumor, intravasation and adhesion to vascular endothelium that finally enables metastases. Altered glycosylation is one of the common features of tumor tissues and plays a vital role in the functional changes of many glycoproteins. It contributes to higher metastatic potential and poor prognosis [1]. All glycosylated molecules displaying alterations during the malignant transformation have potential application as cancer biomarkers [2, 3]. Mucins represent a prime example of glycoproteins expressing abnormal glycosylation pattern in cancer, particularly O-linked Tn

(GalNac α -Ser/Thr) and T (Gal β 1-3GalNAc) antigens and their sialylated forms that were suggested as targets for the design of anti-cancer immunotherapies [4]. Elevated expression of membrane-bound mucins MUC1, 4, and 16 was observed in various cancers [5]. Loss of branched glycans at MUC1 and MUC4 molecules leads to changes in intracellular signaling, impacting multiple processes, including proliferation and migration, mediated through modulation of ligand-receptor interactions. Glycans associated with mucins expressed by tumors can bind to receptors on the surface of dendritic cells, NK cells, and macrophages, which leads to immunosuppression [6]. The involvement and impact of glycosylation in cancer immunology are still somewhat



overlooked. The body of evidence suggests that glycosylation forms an important part of the protein molecule which may contribute, even in a decisive way, to its functions.

Carbonic anhydrase IX (CAIX) is an important transmembrane carbonic anhydrase isoenzyme predominantly expressed in tumors. Its transcription is induced by hypoxia-inducible factor HIF-1, and CAIX is widely expressed in many different carcinomas [7]. CAIX is considered a hypoxia biomarker and a prognostic indicator of specific cancer types [8]. CAIX molecule consists of extracellular catalytically active CA domain N-terminally elongated by proteoglycan-like (PG) domain. The remaining parts of the molecule are a transmembrane domain and a short intracellular tail. Hilvo et al. describe two sites of the glycan attachment for the CAIX molecule. The N-glycosylation site in the CA domain (Asn346) bears a high-mannose glycan structure and O-glycosylation at Thr115 conjugated with O-linked di-, tri-, or tetra-saccharide [9]. Described O-glycosylation site lies in close proximity to the PG domain.

Except for those two short glycan chains, CAIX is modified by glycosaminoglycan polysaccharide chains (GAG) at Serine54 (Ser54), specifically chondroitin and heparan sulfate, forming a high-molecular weight CAIX variant HMW-CAIX [10]. This glycosylation makes CAIX a part-time proteoglycan that can exist in the HMW-CAIX form, typically in the 70–100 kDa size range (under reducing conditions) with GAG modification or in 54/58 kDa form without it. Combined enzymatic digestion of HS and CS chains led to the complete disappearance of the HMW-CAIX form with increased 54/58-CAIX form. The presence of GAG chains on CAIX stimulates cell aggregation as demonstrated by the formation of tight 3D cell aggregates. GAG conjugation negatively regulates CAIX internalization by the caveolin route due to the increased association of CAIX with attached GAG chains with membrane lipid rafts stabilized by caveolin-1 [10].

In cancer progression, CAIX plays an important role as it is involved in the regulation of pH homeostasis, which is essential for the survival of cancer cells with changed metabolism producing more acidic products [11]. Through interactions with β -catenin, CAIX disrupts E-cadherin-mediated adhesion contacts and reduces intercellular adhesion [12]. CAIX translocates to the leading edge of lamellipodium during the migration of cancer cells and participates through cooperation with bicarbonate transporters in the generation of the pH gradient necessary for cell migration [13]. CAIX is also involved in focal adhesion in migrating as well as non-migrating cells, which is important in metastatic processes including intravasation and extravasation [14].

Despite all the information covering various aspects of CAIX features and functions, the data on the contribution of glycan structures to CAIX properties and functions still need to be completed. The main focus of the present study is to investigate the role of glycans in the known CAIX functions. The glycosylation process is often changed during cancer

progression and under hypoxic conditions, and attached glycans often endow such modified proteins with new abilities for interaction, growth factor sequestration, adhesion, etc. As CAIX presents an important hypoxia marker, promising prognostic marker, and possible therapeutic target, it is critical to understand how glycan structures attached to CAIX modify its properties and functions. We intend to provide insights into the impact of glycan modifications of CAIX on pro-survival and pro-metastatic processes in which CAIX protein is involved. GAG chains are characterized by a larger size in comparison to N- or O-glycans and their effect on the functional characteristics of a protein is dominant, therefore, we are particularly focused on differences between GAG modified and core CAIX protein abilities. Our results show that various cell lines derived from different, or even the same, tumor type express the HMW form of CAIX to a different degree while the core protein form always prevails. However, data gained from C33 and MDCK transfectants unable to attach GAG chains prove the importance of this modification for metabolon formation, adhesion, migration, and signaling.

Materials and methods

Cell cultures. MDCK, C33 cells, and their transfected derivatives were grown in a DMEM medium supplemented with 10% fetal calf serum (Lonza BioWhittaker) and 40 μ g/ml gentamicin (Lek Slovenia) at 37°C in the air with 5% CO₂. The same cultivation conditions were applied to tumor cell lines (RKO, HT29, SW620, BxPC3, JIMT-1, 8-MG-BA, 42-MG-BA, A549, HCT116, BT20, HeLa, SiHa). Hypoxic treatments were performed in an anaerobic workstation (Ruskinn Technologies) in 2% O₂ (1% or 0.5% O₂), 2% H₂, 5% CO₂, 91% N₂ (92% or 92.5% N₂) at 37°C.

Cloning and transfection. *In vitro* mutagenesis of CAIX at the site of N-, O-, and GAG glycosylation was performed by PCR using pSG5C-CAIX plasmid and following primers: N346S 5'-tggactgtgtttgccagacagtg-3', N346A 5'-cactgtctgggcaaacacagtcca-3', T115S 5'-gatctactctgttggagctcct-3', T115A 5'-aggagcctcaacagcaggtagatc-3', SS-AA 53-54S 5'-ggaggaggcgtctgtgggaagatg-3', SS-AA 53-54A 5'-catcttccccagcgcctcctcc-3'. C33 and MDCK cells constitutively expressing CAIX or its mutated variants were prepared by co-transfection of pSG5C-CAIX, pSG5C-N346, pSG5C-T115, or pSG5C-53-54 plasmids and pSV2neo in a ratio 10:1 using TurboFect™ *in vitro* Transfection Reagent (Fermentas). A mixture of clones was obtained by Dynabeads M-450 Tosylactivated (Invitrogen) as described previously [14]. CAIX expression was analyzed by flow cytometry, western blotting, and immunofluorescence.

Western blotting. Western blotting was performed as described earlier [15]. Membranes were probed with following antibodies: M75 hybridoma medium (1:3 in 5% non-fat dry milk with 0.2% Nonidet P40 in PBS, 1 h, RT) [16]; anti- β -actin (#3700S, Cell Signaling, 1:5000 in 3% BSA in TBS-T buffer, 1 h, RT); FAK (#3285, Cell Signaling,

1:1000 in 1% BSA in TBS-T buffer, 1 h, RT); pFAK (#8556, Cell Signaling, 1:500 in 1% BSA in TBS-T buffer, 1 h, RT); pJNK1/JNK2 (#44-682G, Invitrogen, 1:500 in 1% BSA in TBS-T buffer, 1 h, RT); polyclonal goat anti-mouse immunoglobulins/HRP or polyclonal goat anti-rabbit immunoglobulins/HRP (PO447, PO448, DAKO, Denmark, 1:5000 in 5% non-fat dry milk with 0.2% Nonidet P40 in PBS, 1 h, RT).

Enzyme-linked immunosorbent assay (ELISA). For an assessment of membrane and total CAIX, the cells seeded in a 96-well plate were allowed to adhere overnight. After 48 h cultivation in normoxia or 2% hypoxia, half of the wells with cells was fixed with ice-cold methanol for 5 min at -20°C and afterward, all of the cells were incubated in peroxidase-conjugated anti-CAIX antibody M75 diluted 1:10000 in 10% DMEM for 3 h. Incubation in peroxidase substrate ortho-phenylene diamine followed by spectrophotometric measurement was used to determine the amount of bound antibody.

Detection of CAIX in culture media was performed by sandwich ELISA using V/10 [17] capture monoclonal antibody (10 $\mu\text{g}/\text{ml}$) specific for the CA domain [18]. For shedding activation, cells were treated with 20 μM phorbol-12-myristate-13-acetate (Sigma-Aldrich, MO, USA) for 4 h at 37°C [19] after their prior cultivation in normoxia or 2% hypoxia.

Flow cytometry for determination of the CAIX internalization. Cells seeded on 6 cm Petri dishes were incubated in 1% hypoxia for 48 h. Afterward, cells were rinsed with PBS and incubated with antibody VII/20 for 30 min at 4°C . One set of Petri dishes with the cells was then rinsed two times with PBS and a part of them was incubated in an acid strip solution for 10 min at RT and rinsed two times in PBS. Afterward, all the cells of the set were trypsinized, centrifuged for 10 min at $415\times g$, and resuspended in PBS. Consequently, cells were fixed by the gradual addition of 70% ice-cold ethanol, while stirring and incubated at -20°C for 1 h. After the fixation step, the cells were centrifuged at $740\times g$ for 10 min, resuspended in PBS, and rehydrated for 5 min at RT. After another centrifugation step at $740\times g$ for 10 min, cells were incubated in secondary anti-mouse antibody Alexa-Fluor 488 for 30 min. Afterward, cells were washed with PBS three times and analyzed by Guava EasyCyteHT (Millipore). After incubation in antibody VII/20 at 4°C , the second set of Petri dishes with the cells was rinsed two times in PBS, and incubated for 3 h at 37°C with a fresh 10% DMEM. Consequently, cells were treated similarly to the first set of Petri dishes with the cells. Data were analyzed by Cytosoft 5.2 software Guava ExpressPro.

Measurement of extracellular pH. pH of a culture media was measured after 24 and 48 h of hypoxic incubation by a special microelectrode (Mettler Toledo, InLab[®] Micro) designed for small volumes. Changes in pH were determined as ΔpH per 24 h and normalized to the concentration of proteins.

Immunofluorescence assay. Cells grown on glass coverslips were gently washed with PBS and fixed in ice-cold methanol at -20°C for 5 min. Nonspecific binding was blocked by incubation with PBS containing 1% BSA for 30 min at 37°C . Cells were then incubated with M75 antibody (5 $\mu\text{g}/\text{ml}$) diluted in a cultivation medium for 1 h at 37°C followed by anti-mouse Alexa Fluor[®] 488-conjugated antibody (Invitrogen, CA, USA) diluted 1:1000 in the blocking buffer for 1 h at 37°C . The nuclei were stained with DAPI (Sigma-Aldrich, MO, USA). Finally, the coverslips were mounted onto slides in the Fluorescent Mounting Media (Sigma-Aldrich, MO, USA), and analyzed by the confocal laser scanning microscope Zeiss LSM 510 Meta.

Adhesion assay. Cells (8×10^5) were seeded, allowed to adhere overnight, and incubated in 2% hypoxia for 48 h. 24-well plates were pre-coated with collagen (isolated from rat tails, diluted to 10 $\mu\text{g}/\text{ml}$, incubated at 4°C overnight) and fibronectin (Sigma, isolated from human plasma, diluted 1:100 in PBS, incubated for 1 h at RT). After pre-coating, all the plates were washed firmly with PBS and blocked with 1% BSA diluted in PBS for 1.5 h at 37°C . During a blocking process, a fresh medium with DiO-C18 (7.5 $\mu\text{g}/\text{ml}$, Invitrogen) was substituted into cells for 45 min incubation at 37°C . Cells were then washed four times with PBS, trypsinized, and seeded on washed and blocked pre-coated plates ($2.5\times 10^5/\text{well}$). Cells were allowed to adhere for 20 or 40 min, washed three times with PBS, and analyzed for fluorescence signal intensity.

To study the process of cell spreading hypoxically pre-incubated (2% O_2 , 48 h) MDCK-CAIX, MDCK-T115, and MDCK-N346 cells in 10% DMEM were seeded in collagen pre-coated 12-well plate. After placing the plate into the incubation chamber (37°C , 21% O_2 , 5% CO_2) only single unspread and round cells were selected and monitored with a Zeiss Cell Observer System. Time-lapse imaging was managed by Axiovision 4.8 software, using the multidimensional acquisition.

Surface plasmon resonance assay. Protein-protein interaction analysis was carried out at 25°C with the BIAcore 2000 system (Biacore[™] T200, GE Healthcare) using HBS-EP buffer (10 mM HEPES, 150 mM NaCl, 3 mM EDTA, pH 7.4, 0.05% v/v Tween). Rat tail collagen I at the concentration of 100 $\mu\text{g}/\text{ml}$ in 10 mM sodium acetate buffer, pH 5.0, was covalently coupled to a CM5 chip (Biacore) using an Amine Coupling Kit (Biacore) at a flow rate of 10 $\mu\text{l}/\text{min}$ according to the manufacturer's protocol. Purified and concentrated CAIX-SBP [20] was used for single-cycle mode analysis. A solution of 21.88 nM CAIX-SBP (streptavidin binding protein) was perfused over the immobilized collagen at a flow rate of 10 $\mu\text{l}/\text{min}$ in HBS-EP running buffer (contact time 2 min), and the resonance changes were recorded. Regeneration of the collagen surface was achieved by running 4M MgCl_2 at the flow rate of 30 $\mu\text{l}/\text{min}$, 30 s with a stabilization period of 3 min. The sensorgrams were obtained and normalized by subtracting the background signals from the

collagen. Sensorgrams were analyzed using BIAcore 2000 evaluation software 3.0.

Migration and invasion assay. The xCELLigence cell index impedance measurements were performed using the CIM-Plate (Accela) placed in a humidified incubator at 37 °C or in an anaerobic work-station (Ruskinn Technologies) in a humidified atmosphere containing 1% O₂ at 37 °C according to the instructions of the supplier (Roche, Basel, Switzerland). Cells were preincubated in hypoxia and starved overnight in DMEM with 0.5% FCS. Cells (4×10⁵/well) were seeded in quadruplicates and their cell index was monitored every 15 min for 100 h. Invasion assay was done similarly using the Matrigel coating in the top chamber.

Wound healing assay. Cells (8×10⁴/well) were seeded in ImageLock 96-well plates (Essen BioScience, UK), allowed to adhere, and then transferred to 1% hypoxia. After starvation in DMEM with 0.5% FCS overnight, confluent layers were wounded with a wound-making tool (Essen Bio-Science, UK) and washed twice with PBS. The migration was run in 0.5% FCS/DMEM with/without HGF (20 ng/ml). Images were taken every two hours for the next 48 h in the IncuCyte ZOOM™ Kinetic Imaging System (Essen BioScience, UK). Migration was evaluated by IncuCyte ZOOM™ 2013A software (Essen BioScience, UK) based on the relative wound density measurements and expressed as means of two independent experiments performed in sextaplicates ± SD.

Proteome Profiler™ Array, Human Phospho-Kinase Array Kit. This array (R&D systems) was conducted on stable transfected C33 cells expressing wild type CAIX and CAIX GAGm. Cells were cultured under the same cultivation conditions (48 h, 1% hypoxia). Cell lysates were prepared and subsequently applied to Kinase Array membranes. Proteins were quantified by measuring the accumulated pixel density of the individual spots and adjusted based on reference spots using the ImageJ software. The whole procedure and analysis were performed according to the manufacturer's instructions.

Quantitative PCR (qPCR). Total RNA was isolated using RNeasy Plus Mini Kit (Qiagen, Hilden, Germany), and reverse transcription of 1 µg RNA for each sample was performed with the High-Capacity cDNA Reverse Transcription kit (Applied Biosystems, CA, USA). qPCR was carried out using Maxima SyberGreen PCR Master mix (Thermo Fisher Scientific, MA, USA), gene-specific primers listed in Supplementary Table S1 and ran for 10 min at 95 °C for initial denaturation followed by 40 cycles of 95 °C for 15 s and 60 °C for 1 min. Sample CT values were normalized to β-actin. Relative expression was calculated using the ΔΔCT method. All amplifications were performed in triplicates. Results were calculated from two independent experiments.

Results

Basic characterization of CAIX protein without N or O-linked glycosylation and the impact of lost glycans on CAIX function. To study the effect of glycosylation changes

on the basic characteristics of CAIX protein and cell properties, we prepared cells MDCK and C33 stable transfected with wild type CAIX (denoted MDCK-CAIX or C33-CAIX) and CAIX with mutations in glycosylation sites Asn346 (MDCK-N346 or C33-N346) and Thr115 (MDCK-T115 or C33-T115) using pSG5C plasmids and magnetic beads-coupled with CAIX-specific antibody M75 for the selection of CAIX positive cells and maintained at above 90% of CAIX positive cells. Immunofluorescence analysis (Figure 1B) showed that plasma membrane localization of CAIX is also maintained in cells expressing mutated variants of CAIX protein. This result was confirmed by ELISA assay comparing the total CAIX signal in fixed cells to the membrane-bound CAIX signal in live cells (Figure 1C). We determined a comparable ratio of the membrane-localized CAIX protein in wild type and mutated CAIX-expressing cells, in both cell types. To evaluate the ability of CAIX protein variants to form oligomers, we performed the western blot analysis (Figure 1D). Oligomerization in native (non-reducing) conditions as well as the typical two-band pattern of molecular weight 54/58 kDa was maintained in all of the transfected cell lines. We also observed an expected shift of a monomeric form of CAIX protein in MDCK-N346 and C33-N346 cell lysates in reducing as well as non-reducing PAGE (Figure 1D), which corresponds to the loss of N-glycan structure in MDCK/C33-N346 mutated cells. Membrane localization is the main prerequisite for the involvement of CAIX in the regulation of tumor cell pH, which belongs to the key factors contributing to tumor cell survival and metastasis. As the CAIX activity is linked to the acidification of the extracellular environment, we measured the pH of a culture media of cell monolayers cultured in 2% hypoxia for 24 h and 48 h. The ability of transfected MDCK cells to acidify culture media was assessed as a difference in media pH (ΔpH) during 24 h normalized to the total protein concentration. We observed no significant changes in ΔpH among the studied samples (Figure 1E).

In our previous works, we described the involvement of CAIX in the process of focal adhesion of cells to a substrate and in the spreading of quiescent cells. As glycans are among the most important structures involved in the adhesion processes, we studied the capacity of our transfectants to adhere to selected components of the extracellular matrix - collagen and fibronectin. We employed MDCK cells which are more suitable for studying the initial adhesion of cells to a substrate. We observed no significant changes in the adhesion of CAIX-expressing MDCK cells to fibronectin but in the case of collagen, both of the transfectants expressing mutated CAIX forms (MDCK-N346 and MDCK-T115) showed a reduced adhesion capacity in comparison to MDCK-CAIX cells (Figures 1F, 1G). Figure 1H shows representative pictures of the morphology of MDCK-CAIX, MDCK-N346, and MDCK-T115 cells during the steps of adhesion and spreading at given time points. In timepoint 0 at the beginning of the experiment, all analyzed cells were round. Morphology analysis at the later time points showed

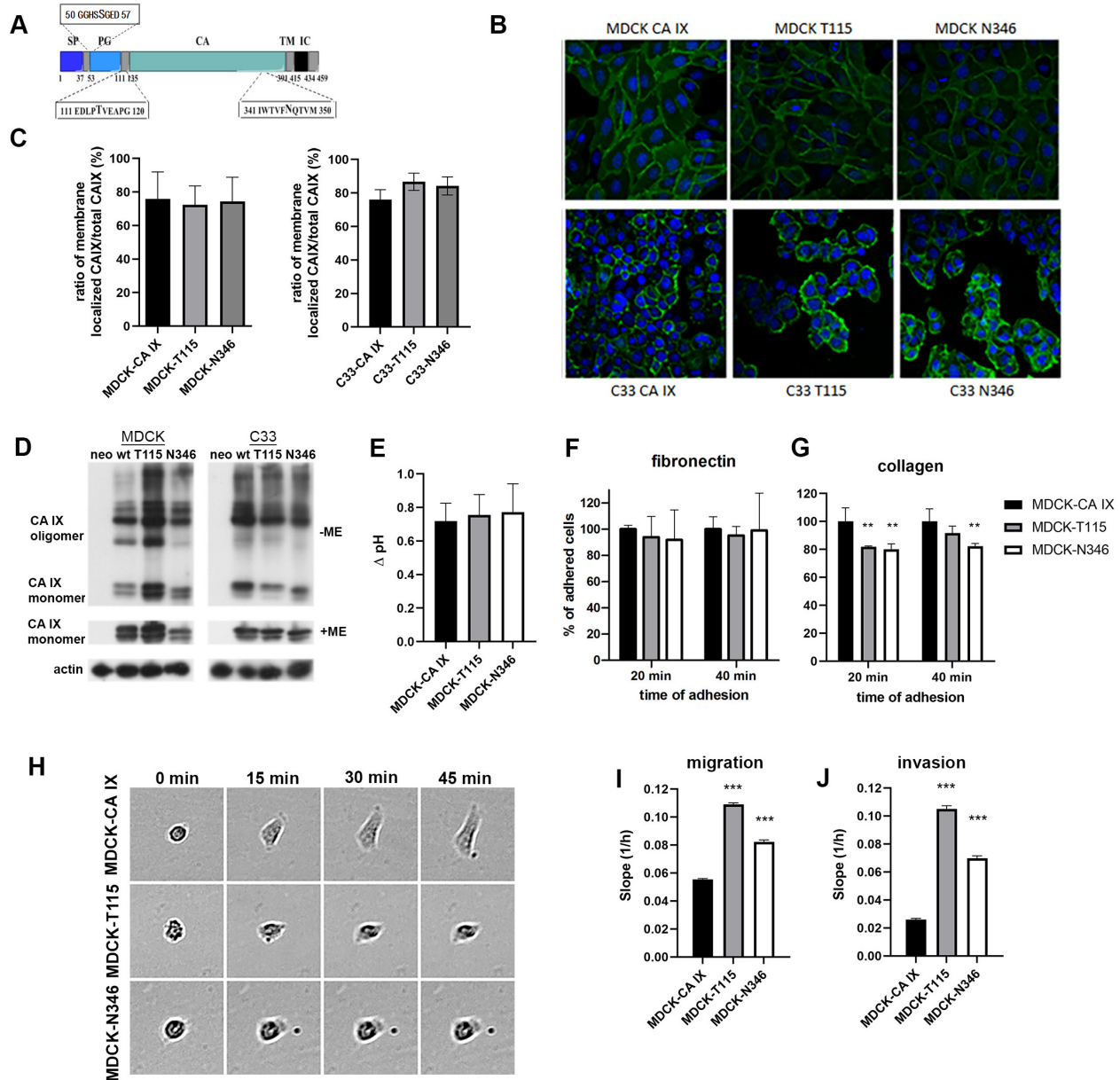


Figure 1. Impact of N or O-linked glycosylation loss on CAIX function. A) Schematic picture of CAIX molecule, which is composed of signaling peptide (SP), proteoglycan-like (PG) domain, catalytic (CA) domain, transmembrane (TM) region, and intracellular (IC) tail. Sites of glycan modification are displayed in amino acid positions 115 and 346. The site of GAG modification is shown at Ser54. B) Immunofluorescence analysis of MDCK/C33 cells expressing wild type CAIX and CAIX with mutations at T115 and N346 (CAIX-green, DAPI stained nuclei-blue), images were acquired by Zeiss LSM 510, 40 \times objective. C) ELISA comparing the membrane-bound amount of CAIX in live cells and the total amount of CAIX in fixed cells. The graph gives means \pm SD of membrane/total CAIX ratio measured in pentaplicates. Possible differences were evaluated by ANOVA and found non-significant. D) Representative western blot analysis of MDCK/C33 cell lysates from cells expressing wild type (wt), T115, and N346-mutated CAIX separated under non-reducing (-ME) and reducing (+ME) conditions. Neo denotes cells transfected with an empty plasmid. E) Acidification of extracellular pH by MDCK cells expressing wild type, N346, and T115-mutated CAIX cultured in 2% hypoxia for 48 h. Acidification of the media was expressed as Δ pH during 24 h and the results were normalized to total protein concentration. The experiment was repeated 4 times in triplicates. The graph displays means \pm SD. No significant changes in Δ pH were observed among tested cell lines. F, G) Adhesion of MDCK cells expressing wild type, N346, and T115-mutated CAIX to fibronectin and collagen. Cell adhesion is expressed as a percentage of adhered cells when compared to MDCK-CAIX cells (set as 100%). Values are expressed as mean \pm SD of two independent experiments performed in duplicates, ** p <0.01. H) Representative pictures of the morphology of selected MDCK cells expressing wild type, N346, and T115-mutated CAIX during the process of adhesion and spreading at chosen time points. Images were acquired by Zeiss Cell Observer microscope, 10 \times objective. I, J) Transwell migration and invasion assay performed using the xCELLigence system with MDCK cells expressing wild type, N346, and T115-mutated CAIX. Representative graphs give mean \pm SD of the slopes, measured in quadruplicates, reflecting the migration/invasion rate of the cells during the chemotactic assay. The significance of differences was assessed by one-way ANOVA with Dunnett's multiple comparison post-hoc test, *** p <0.001.

that MDCK-N346 and MDCK-T115 cells spread more slowly in comparison to MDCK-CAIX cells. CAIX is implicated in the migration and invasion processes of tumor cells, but the role of glycans has not yet been investigated. Using the xCELLigence system, the Transwell migration assay showed that the loss of glycan structure at N346 and T115 in both cell types led to increased migration in comparison to the controls (Figure 1I). The loss of glycosylation in N346 and T115 also increased the invasion of MDCK transfectants through Matrigel-coated porous membrane in the invasion assay detected by the xCELLigence system (Figure 1J). Similar results were obtained for C33 cells (Supplementary Figure S1).

Based on our adhesion experiments results, we investigated the possibility of interaction between CAIX and collagen. Single cycle (yes/no) binding assay of purified CA IX-SBP (streptavidin binding protein) and collagen type I was performed by the SPR method. Collagen was immobilized on a CM5 sensor chip under acidic conditions (Supplementary Figure S2), and the interactions between flowing CA IX-SBP and immobilized collagen type I were measured under physiological conditions. The sensorgram in Figure 2 shows the direct binding between purified CA IX-SBP protein (21.88 nM, pink line) and collagen type I. SBP alone (20 µg/ml, green line) displays no binding capacity. Interaction analysis of CAIX-SBP with collagen after regeneration with 4 M MgCl₂ showed almost the same binding effectivity of CA IX-SBP with collagen as before chip-regeneration (Supplementary Figure S2 lower panel). Dissociation of CA IX-SBP from the collagen was rather slow indicating stable interaction between these two proteins.

Basic characterization and the level of GAG-modified CAIX in tumor cell lines. The PG domain of CAIX includes the site of GAG binding at Ser54 (Figure 1A) where the HS or CS chain can be attached to the molecule [10]. CAIX was confirmed as a “part-time” proteoglycan that can exist in the form with or without GAG modification. To assess the level

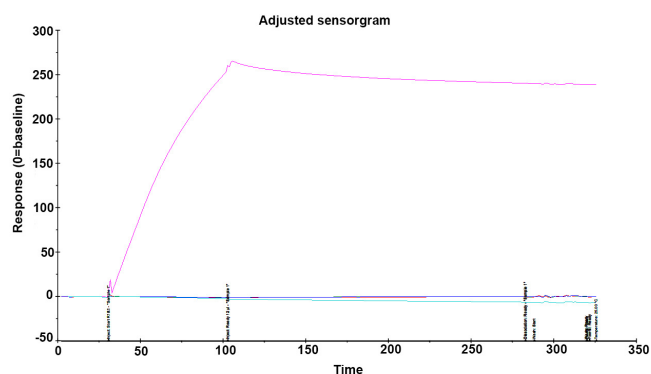


Figure 2. Sensorgram showing the direct binding between CA IX-SBP and collagen type I immobilized on CM5 sensor chip (pink line). Protein-protein interaction analysis was performed at the BIAcore 2000 system.

of GAG-modified CAIX molecule, we analyzed tumor cell lines with various characteristics ranging from less aggressive to very aggressive and metastatic in normoxic and hypoxic conditions. The level of CAIX without GAG was higher in all of the tested cell lines (Figure 3A). For this reason, the parts of the films with high molecular weight CAIX forms were exposed for a longer time in order to enable a comparison of the levels of GAG-modified CAIX in the various cell lines. The ratio between 54/58 kDa CAIX form and HMW GAG-modified CAIX form differed considerably among compared tumor cell lines (Figures 3A, 3B). We observed a high level of GAG modification in glioblastoma cell lines 42-MG-BA and 8-MG-BA, as well as in breast cancer cell line JIMT-1, colorectal cancer cell lines RKO, HT29, and SW620, and pancreatic cell line Colo357. Moderate GAG modification was exhibited by cervical cancer cell lines SiHa and HeLa, as well as lung adenocarcinoma cells A549. The lowest level of GAG modification was displayed by breast carcinoma cell line BT20, pancreatic BxPC3, PaTu, and colorectal carcinoma cell line HCT116. All tumor cell lines, except HT29, display a strong hypoxic induction of CAIX. We can conclude that the rise of HMW CAIX in hypoxia is connected to the increase of the synthesis of core CAIX protein and the level of GAG modified form is cell-type dependent.

Impact of the GAG modification on protein functions.

To investigate the role of GAG modification of CAIX protein, we also prepared MDCK and C33 cells stably transfected with pSG5C-CAIX plasmid carrying mutations in Ser53-54 that causes a loss of HS/CS glycan structure from the CAIX molecule (denoted as MDCK-GAGm and C33-GAGm, Figure 4A). Immunofluorescence analysis of prepared mutants confirmed that the loss of GAG structure does not influence membrane localization of CAIX protein (Figure 4B) [10]. The level of membrane-localized protein in both types of transfectants is comparable (Supplementary Figure S3).

Measurements of the extracellular pH of culture media showed increased acidification of MDCK-GAGm cell monolayer in comparison to MDCK-CAIX cells (Figure 4C) cultured in 2% hypoxia for 48 h. During pH regulation and subsequent extracellular acidification, CAIX cooperates with bicarbonate transporters, forming a transport metabolon that enhances the transport of bicarbonate ions through the cell membrane and increases the production of protons in the extracellular space. Using proximity ligation assay which enables *in situ* detection of protein interactions, we detected an increased formation of a metabolon between CAIX without HS/CS chains and anion exchanger AE2 (encoded by *SLC4A2* gene), which is involved in bicarbonate transport, in C33-GAGm cells compared to control C33-CAIX cells (Figures 4D, 4E).

As proteoglycans are involved in the formation of intercellular contacts, we tested the ability of MDCK-CAIX and MDCK-GAGm cells to form cell-cell contacts and subsequently aggregates during their culture in a suspension at a rotational shaker. The aggregation assay showed that cells

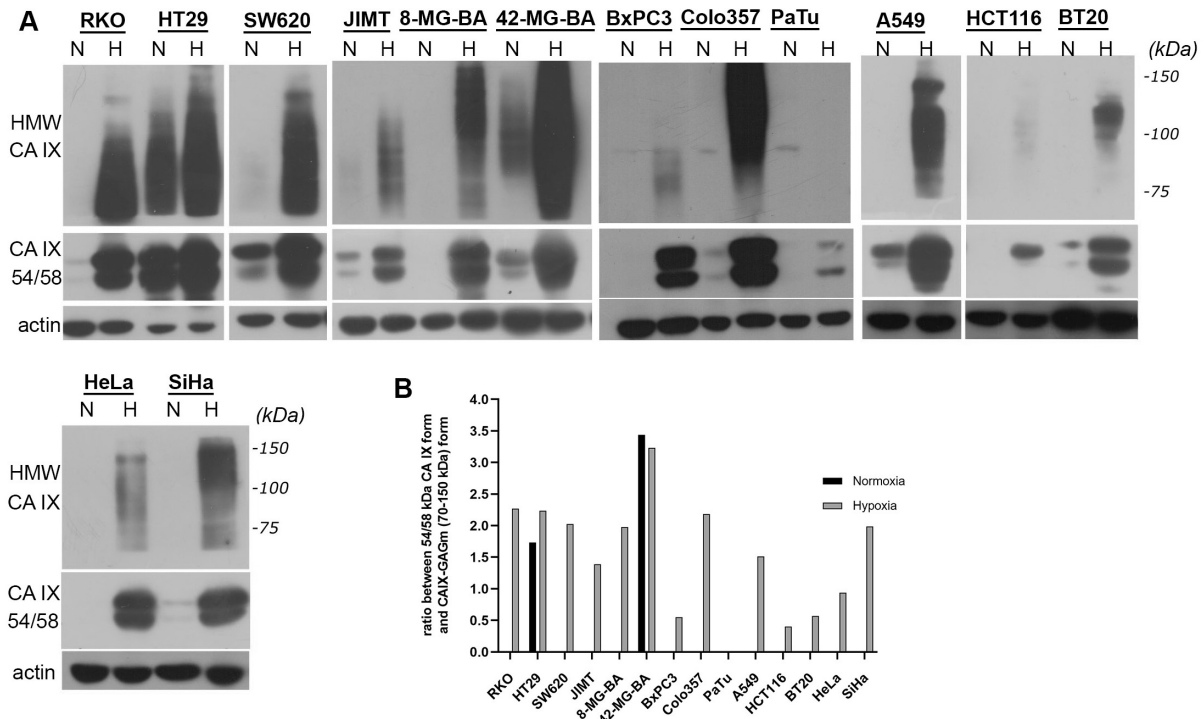


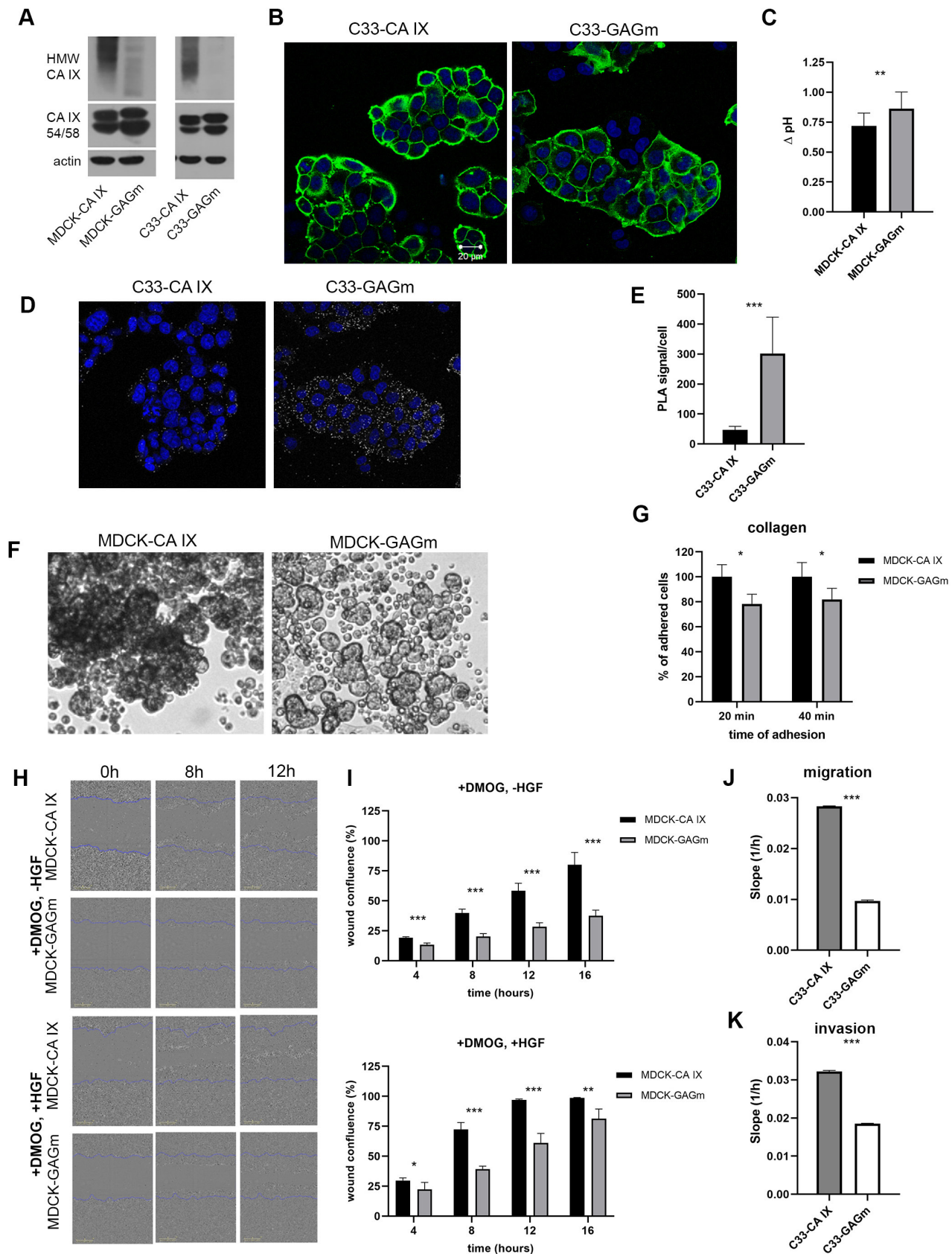
Figure 3. GAG-modified CAIX expression in tumor cell lines. **A**) Western blot analysis of 54/58 kDa form and high molecular weight forms (70–150 kDa, HMW) of CAIX protein expressed in cell lines derived from carcinoma of various origins cultured under normoxic and hypoxic conditions. **B**) Graph of the ratio between the HMW form of CAIX and the core form of CAIX (54/58 kDa) without the GAG modification. The ratio does not provide absolute values but serves as a tool for comparing the share of GAG-modified HMW forms of CAIX among different cell lines. Western blots were analyzed by the ImageJ program (Analyze Gels tool).

expressing CAIX without GAGs exhibited diminished cell-cell contacts and formed smaller aggregates than MDCK-CAIX cells (Figure 4F; Supplementary Figure S4) in accordance with the results of 3D formation assay with U87-MG cells without GAG modification due to the mutation at Ser54 [10]. It indicates that GAG bound to CAIX enhances cell-cell adhesion to form cellular aggregates. Interactions of chondroitin sulfate and heparan sulfate chains with collagen

and other ECM proteins were described, hence we investigated the impact of missing GAG at the involvement of CAIX in the process of cell adhesion to a substrate. When compared to MDCK-CAIX cells, we observed decreased adhesion of MDCK-GAGm cells to collagen (Figure 4G), which was also confirmed in C33 cells (Supplementary Figure S5).

The effect of GAG modification of CAIX on the migration process was evaluated in the wound healing assay using

► **Figure 4.** Impact of the GAG modification on CAIX functions. **A**) Western blot analysis showing the loss of the high molecular weight (HMW) form of CAIX in GAGm cells. **B**) Immunofluorescence analysis of C33 cells expressing wild type and GAGm variant of CAIX (CAIX-green, DAPI stained nuclei-blue), images were acquired by Zeiss LSM 510, 40× objective. **C**) Measurement of the ability of MDCK cells expressing wild type and GAGm CAIX cultivated in 2% hypoxia for 48 h to acidify the culture media. Acidification of the media was expressed as Δ pH during 24 h and the results were normalized to total protein concentration. The experiment was repeated 4 times in triplicates. The graph gives the values of means \pm SD (** p <0.01). **D**) *In situ* detection of interaction between CAIX and AE2 in C33 cells expressing wild type CAIX (C33-CAIX) and CAIX-GAGm cells using the Proximity ligation assay. An increased formation of metabolon, which is visualized as white dots on cellular membranes, was observed in C33-GAGm cells in comparison to control cells. Nuclei were stained with DAPI (blue). Images were taken at Zeiss LSM 510, 40× objective. **E**) Graph quantifying the PLA signal. **F**) Representative images of cell aggregates. MDCK-GAGm cells exhibited diminished cell-cell contacts and formation of smaller aggregates in comparison to MDCK wild type cells. Images were taken at Zeiss Axiovert 40 CFL, 10× objective. **G**) Adhesion of MDCK cells expressing wild type and CAIX-GAGm to collagen. Cell adhesion is expressed as a percentage of adhered cells when compared to MDCK-CAIX (set as 100%). Values are expressed as mean \pm SD of two independent experiments performed in duplicates. **H**) Representative images of the wound healing assay performed using the IncuCyte system with MDCK wild type and GAGm cells in hypoxic conditions (+DMOG). **I**) The graphs of the wound confluence at selected time points. The confluence of 100% MDCK means that the wound was healed, i.e., completely covered by cells. **J**, **K**) Transwell migration and invasion assay performed using the xCELLigence system with C33 cells expressing wild type and CAIX-GAGm. Particular slopes in representative graphs from one experiment illustrate the migration rate of the cells. **C**, **E**, **J**, **K**) Significance of differences was evaluated by Student's t-test in comparison to control MDCK-CAIX or C33-CAIX cells, and in the case of panels **G**, **I** at separate time points, * p <0.05, ** p <0.01, *** p <0.001.



the IncuCyte system (Figure 4H). We noticed the decreased migration of MDCK-GAGm cells pre-incubated in 1% hypoxia. Migration of MDCK-GAGm cells was reduced in comparison to MDCK-CAIX cells during wound closure in normoxic conditions (data not shown), as well as in hypoxia (DMOG treated cells) in the presence or absence of hepatocyte growth factor (Figure 4I). As expected, cells treated with HGF migrated faster but a difference in migration rate of cells with CAIX with and without GAG modification was preserved. The difference in cell migration rate was also confirmed by the Transwell migration assay using the xCELLigence system when cells migrate through a porous membrane towards a chemoattractant. The migration of C33-GAGm cells was reduced (Figure 4J). Similar results were obtained in the invasion assay in which the top of a porous membrane was coated with Matrigel and the cells have to proteolytically cleave the ECM layer to be able to migrate towards chemoattractant in the lower chamber (Figure 4K). The results of migration and invasion assays employing MDCK-GAGm and MDCK-CAIX are presented in Supplementary Figure S6.

Loss of the GAG modification reduces phosphorylation of selected protein kinases and transcription factors and leads to downregulation of the EMT signature. In order to identify possible changes in signaling pathways due to the loss of CAIX GAG structures, we used the Proteome Profiler Array, Human Phospho-Kinase Array Kit that enables the determination of the phosphorylation level of various protein kinases and their substrates. C33 cells were cultured in hypoxic conditions (1% O₂) for 48 h and protein lysates were used for the determination of CAIX-dependent differences between phosphorylation profiles of C33-CAIX and C33-GAGm cells. A comparison of the phosphorylation level of selected kinases and their substrates (Figure 5A) showed the most prominent reduction in phosphorylation of c-Jun at S63 (to 52%) in C33-GAGm cells compared to C33-CAIX cells. A relevant decrease was observed also in phosphorylation of p38 α kinase at T180/Y182 (to 65%), focal adhesion kinase (FAK) at Y397 (to 72%), and a reduced protein level of HSP60 (to 62%) in C33-GAGm cells (Figure 5B). Immunoblotting of protein lysates of hypoxically cultured C33 cells expressing CAIX without GAG chains confirmed reduced phosphorylation of FAK kinase. Phosphorylation of FAK-Y397 was reduced to 30% of the control cells evaluated by densitometry of western blotting (Figure 5C). Further, we investigated the expression of EMT-associated genes whose expression is regulated by the c-Jun transcription factor. The strong reduction was proved for *Snail* and *Twist* as direct downstream targets of c-Jun (Figure 5D). Importantly, *MMP14*, another c-Jun target gene was substantially downregulated, as well. The most profound reduction of mRNA level was observed for fibronectin, whose transcription is regulated by all three transcription factors c-Jun, *Snail*, and *Twist* the levels of which were decreased in C33-GAGm cells.

Internalization and ectodomain shedding. Immunofluorescence analysis of the internalization induced by VII/20 antibody, which proceeds by the clathrin endocytic pathway [21] in MDCK-GAGm and C33-GAGm cells, showed a similar pattern when compared to control cells (Figure 6A). This result was also confirmed by flow cytometry analysis of CAIX internalization. Loss of the GAG structure has no impact on CAIX internalization induced by VII/20 antibody (Figure 6B). Another post-translational process regulating the membrane level of CAIX protein is the shedding of the extracellular part of the CAIX molecule mediated by enzymes – metalloproteases. Shed CAIX ectodomain is detectable in the fluids of cancer patients and acts as a promising tumor marker, and this soluble form of the protein may play a role in paracrine signaling. Using a sandwich-type ELISA, we found out that the level of CAIX ectodomain in culture media of MDCK-GAGm cells was higher in hypoxia in basal (by 80%), as well as PMA (phorbol-12-myristate-13-acetate)-activated conditions (by 18%). PMA is used as a shedding inducer acting through the protein kinase C pathway and it was also identified as a strong inducer of ADAM17, a disintegrin and metalloproteinase 17 responsible for the cleavage of CAIX from the cell surface [19, 22]. In normoxia, the level of ectodomain shedding of MDCK-GAGm cells was similar to MDCK-CAIX (Figure 6C). These findings were also confirmed in C33 transfectants (Supplementary Figure S7).

Discussion

Glycosylation is the most frequent post-translational modification providing a very diverse and complex way of altering protein structure. Glycan synthesis does not follow a strict template. It depends on the wide range of nucleotide sugar transporters, glycosyltransferases, glycosidases, and enzymes that further modify glycan chains, such as sialylation, fucosylation, and sulfation. Cancer cells display alterations in the glycosylation pattern of proteins, which respond to microenvironmental conditions and contribute to tumor growth and metastasizing. Glycans affect cellular signaling, cell-cell, cell-matrix adhesion, and migration processes, and directly mediate interactions between receptors and their ligands [23].

Carbonic anhydrase IX belongs among the key enzymes of the adaptive microenvironmental machinery of tumor cells. Its expression in tumor tissues is linked to poor prognosis, tumors' aggressive character, and radio- and chemo-resistance. Despite its involvement in several processes supporting tumor growth and metastasizing, the role of glycan structures of CAIX in cellular processes has yet to be fully elucidated, and publications concentrated mainly on the identification of glycan attachment sites and types of attached glycan structures [9, 10, 24].

To examine CAIX glycan functions, we prepared MDCK and C33 cells stably expressing the CAIX protein with

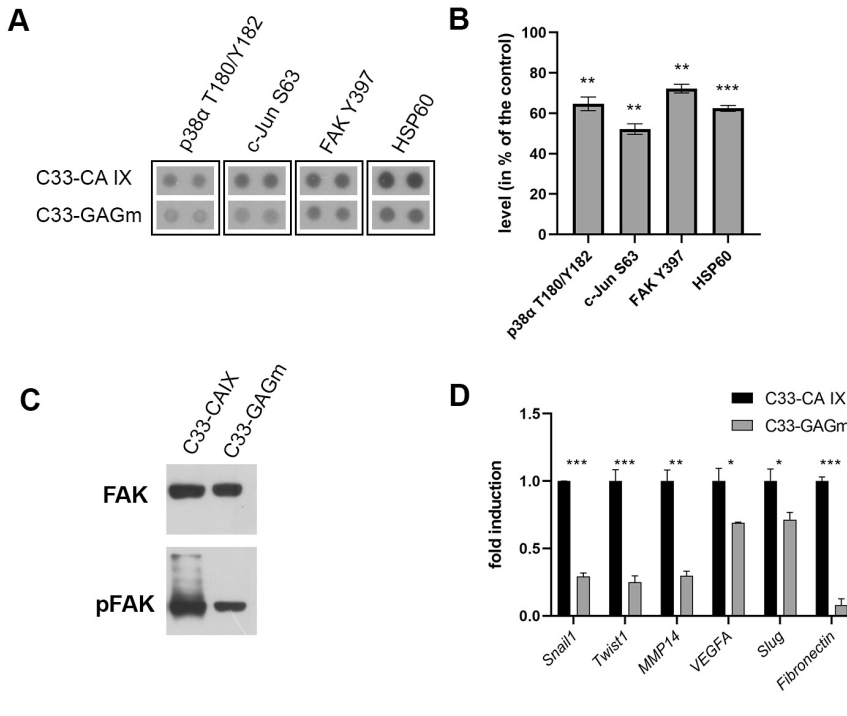


Figure 5. Impact of the GAG modification on phosphorylation levels of selected protein kinases and EMT-related genes. **A)** Protein kinases and their targets with the most changed phosphorylation profiles in C33-CAIX and C33-GAGm cell lysates, determined by the Proteome Profiler Array, Human Phospho-Kinase Array Kit: p38α T180/Y182, c-Jun S63 FAK Y397, HSP60. **B)** Quantification of Proteome Profiler Array results. The experiment was performed in duplicates. Data normalized on protein concentration are expressed as mean ± SD, levels measured in control C33-CAIX cells were set as 100%. **C)** Western blot of phosphorylation and total levels of FAK kinase of C33-CAIX and C33-GAGm cells cultured in hypoxia. **D)** Evaluation of mRNA levels of selected EMT-related genes in C33-CAIX and C33-GAGm cells cultured in hypoxia.

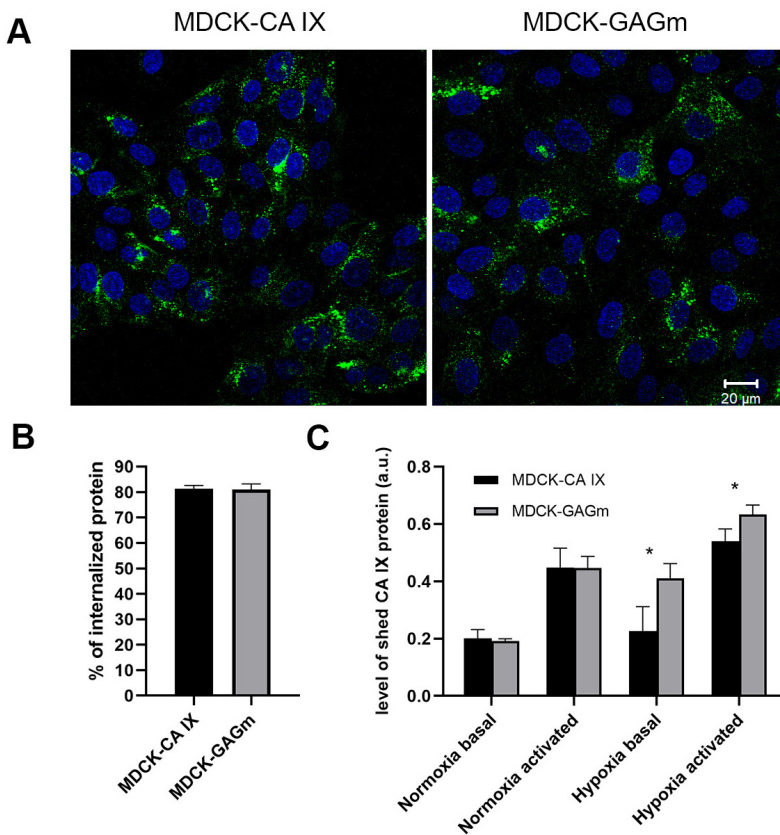


Figure 6. Internalization and ectodomain shedding of GAGm cells. **A)** Representative images of CAIX internalization induced by antibody VII/20 in MDCK-CAIX and GAGm cells. Cells were incubated with antibody VII/20 for 4 h at 37 °C to allow internalization. The images show the internalized intracellular CAIX, acid strip before fixation was used to remove the extracellular antibody. CAIX signal is green, nuclei were stained with DAPI (blue). Zeiss LSM 510, 40× objective. **B)** Flow cytometry analysis of the CAIX internalization induced by antibody VII/20 in MDCK-CAIX and GAGm cells. The experiment was repeated three times. Data represent means ± SD. **C)** Levels of shed CAIX ectodomain in MDCK-CAIX and GAGm cells determined by ELISA. Data were normalized on total protein concentration and concentration of CAIX. For shedding activation, cells were treated with 20 μM phorbol-12-myristate-13-acetate for 4 h at 37 °C after their prior cultivation in normoxia or 2% hypoxia. The experiment was repeated twice in quadruplicates. All data represent means ± SD, *p<0.05 in comparison to control MDCK-CAIX cells evaluated by Student's t-test.

the mutations in glycan-binding sites, leading to a loss of attached glycans. We can conclude that CAIX proteins without glycan attachment at N346 or T115 sites form oligomers and maintain membrane localization, a prerequisite of CAIX function, and its involvement in pH regulation, adhesion, and migration. The loss of N-glycan and O-glycan structures on N346 and T115 of CAIX in MDCK and C33 cells led to their increased migration rate as well as enhanced invasion ability of mutated cells through Matrigel-coated porous membrane. Adhesion of cells to extracellular matrix or other substrates is a necessary step involved in migration and invasion, which are integral parts of the process of metastasizing. CAIX has been implicated in the adhesion process in quiescent, spreading, and migrating cells [14]. CAIX localizes directly to focal adhesion plaques, where it colocalizes with paxillin, and is also involved in regulating focal contact turnover during migration. Our results show that the loss of CAIX glycan structures at T115 and N346 leads to reduced adhesion of cells to collagen but not to fibronectin. Our measurement using plasmon surface resonance for the first time showed a direct binding between CAIX and collagen, and a relatively slow dissociation of CAIX from the collagen surface indicates a rather strong interaction between these two proteins.

Recently, the protein CAIX was described as a hypoxia-regulated part-time proteoglycan that can exist without GAG chains and in the form containing GAG modification when HS or CS chains are attached at Ser54 [10]. This high molecular weight form of CAIX protein was reported to have 70–100 kDa in two human glioma cell lines, U87-MG and U251-MG. Our data show significant variability in the extent of GAG modification in various tumor cell lines of different origins. However, the core protein without GAG modification always prevails. We can confirm hypoxic induction of the HMW form of CAIX. The composition of GAG chains is cell type-specific depending on the sum of glycosyltransferases and glycosidases involved in their synthesis [25].

To assess the contribution of GAG structures attached to CAIX in cellular processes in which the role of CAIX had been described, we used MDCK and C33 transfectants expressing CAIX protein without the GAG modification. Acidification of the extracellular environment is linked with the pH-regulating function of CAIX and its cooperation with bicarbonate transporters. According to our results, hypoxically preincubated MDCK-GAGm cells showed more acidic extracellular pH of culture media than control MDCK-CAIX cells. Correspondingly, we detected the increased formation of a transport metabolon between CAIX and AE2 in C33-GAGm cells. Metabolon formation increases the ion flux through the plasma membrane and contributes to lower extracellular pH by proton production. Although most CAIX molecules expressed in control cells naturally lack the GAG structure, high molecular weight GAG chains may affect metabolon formation by presenting spatial obstacles.

Heparan and chondroitin sulfate proteoglycans (HSPGNS, CSPGNS) are also implicated in tumor proliferation, migration, invasion, angiogenesis, and metastasis, and CS chains can bind various humoral factors, including fibroblast growth factor, hepatocyte growth factor, brain-derived growth factor [26]. For example, chondroitin chains of melanoma-specific CS proteoglycan (MCSP) in tumor cells bind catalytically inactive matrix metalloproteinase 2 (pro-MMP2) and membrane-type 3 matrix metalloproteinase (MT3-MMP), facilitating their interaction. Removing the pro-MMP2 prodomain by MT3-MMP leads to the generation of active MMP2 necessary for tumor invasion and metastasis [27, 28]. In some cases, HSPGNS and CSPGNS have an opposing roles and act as tumor suppressors. Whether the effect is tumor-promoting or suppressing depends on the cell type and a set of growth factors, and the enzymatic modification of HS/CS chains [29]. In our experiments, the absence of HS and CS chains resulted in a decreased migration of MDCK-GAGm compared to MDCK-CAIX cells pre-incubated in hypoxia in a wound healing test. Similarly, MDCK-GAGm and C33-GAGm cells showed reduced chemotactic migration and invasion through Matrigel. These results indicate that GAG glycosylation promotes CAIX's role in migration and invasion processes. Svastova et al. (2012) demonstrated CAIX-mediated enhancement of cell migration. In addition, the expression of CAIX decreased the required concentration of HGF needed to facilitate migration speed [13]. It is possible that through HS/CS chains, CAIX can sequester HGF and present it to its receptor c-Met, thereby participating in the stimulation of migration and c-Met downstream signalization.

The proteoglycan domain of the CAIX protein is also involved in the process of cell spreading as the addition of the M75 antibody, which binds to a linear epitope in the PG domain, as well as deletion of the CAIX-PG domain [30] resulted in decreased cell spreading [14]. Our findings indicate that HS/CS chains attached to the site in the CAIX-PG domain participate in the adhesion of CAIX-expressing cells to collagen as the number of adhered cells decreased in MDCK-GAGm cells compared to MDCK-CAIX. It is known that pre-incubation of the matrix by HS and CS led to the inhibition of ovarian cancer cells' adhesion to type I and type II collagens [31]. Enzymatic removal of HS and CS chains also reduced cell adhesion. Breast carcinoma cells were sensitive to exogenous heparan sulfate and heparin, which led to increased focal adhesion and spreading of cells to collagen and, at the same time, reduced invasion and matrix degradation [32].

HS and CS chains can influence cell signaling by acting as co-receptors, sequestering growth factors, and interacting directly or indirectly with proteins involved in signaling pathways. Their role as co-receptors for receptor tyrosine kinases (RTKs) in promoting proliferation and tumor growth was documented in carcinoma cell lines originating from ovaries, breast, pancreas, kidney, and liver [33, 34].

Our results of the phosphokinase protein array showed that removing GAG glycosylation from CAIX protein caused a reduction in the phosphorylation of c-Jun, p38 α kinase, and FAK in C33-GAGm cells cultured in hypoxic conditions. Activation of these pathways is associated with migration and invasion processes, which were reduced in cells with the removal of CAIX-GAG glycosylation. Further, phosphoproteins significantly changed in CAIX-GAGm cells are crucial regulators of the EMT phenotype. Actually, EMT markers like *Snail 1*, *Slug*, *Twist*, and *Fibronectin* were diminished in C33-GAGm cells. Specifically, the expression of *Snail*, *Twist*, and *MMP14* is directly regulated by the c-Jun transcription factor, whose phosphorylation at Ser63 is reduced to 52%. It is the c-Jun activation via p38 α -dependent phosphorylation at Ser63 that leads to its binding to the *Snail* promoter thereby inducing *Snail* expression and Snail-dependent migration and invasiveness [35]. Also, c-Jun phosphorylation/activation and dimerization with c-Fos form an active AP1 transcription complex driving *Twist* gene expression and EMT [36]. Subsequently, a decrease in *Snail 1* and *Twist*, two TFs regulating fibronectin expression [37, 38], detected in CAIX-GAGm cells probably led to dramatic fibronectin downregulation. Another downregulated signaling mediated by the removal of GAG chains from CAIX protein is tyrosine phosphorylation of FAK. It is known that CAIX interacts with collagen-binding integrins ($\beta 1$ and $\alpha 2$ subunits) [39]. Integrin binding to collagen increases FAK recruitment and phosphorylation. In addition to the observation of CAIX-promoting adhesion to collagen, we also proved a direct binding of purified CAIX to collagen matrix using the surface plasmon resonance method. We suggest that reduced tyrosine phosphorylation of Tyr397-FAK in CAIX-GAGm cells can be the consequence of reduced interaction between CAIX-GAGm and its integrin partners. Interestingly, another protein markedly reduced in CAIX-GAGm cells was HSP60 that, when localized on the membrane, is able to interact with $\alpha 3\beta 1$ integrin and activate it [40]. This interaction was necessary for the adhesion of breast cancer cells metastasizing into lymph nodes.

A common stress phenomenon of the tumor microenvironment is inflammation. In our experiments, the amount of GAG chains on the CAIX molecule decreased in response to the inflammatory environment (Supplementary Figure S8). Cytokines like IFN- γ , IL-1 α , and TNF α significantly affect cancer-associated mucins MUC1, MUC5AC, and MUC16 glycosylation across different pancreatic cancer cell lines and the response is cell-type specific. Generally, inflammatory cytokines/chemokines can lead to an increase or decrease of glycan levels [41]. Underglycosylation of MUC1 is the early hallmark of tumorigenesis and is associated with cellular invasion, and immune tolerance e.g., by inhibiting T-cell activation or with the differentiation of macrophages to immunosuppressive M2 phenotype [42, 43, 44]. Inflammatory cytokines/chemokines, a source of external signaling from the tumor microenvironment that can alter glycosyl-

ation, could belong to important physiological modulators of CAIX-GAG glycosylation. We also observed that cells adapted to extracellular acidosis (pHe 6.7) reduced GAG glycans on CAIX molecules (Supplementary Figure S9). Through alternating the level of GAG modification on CAIX molecules, cells could react to acidosis, which is another tumor-related phenomenon, and tune pH-regulating activity, as the absence of GAG chains on CAIX increases the formation of CAIX-bicarbonate transporter metabolon, which facilitates intracellular pH buffering (Supplementary Figure S9).

A vital role of CAIX-GAG modification was recently shown by Christianson et al. (2017), who demonstrated that the presence of GAG chains negatively regulates CAIX internalization induced by M75 antibody through an increased association with caveolin-1 stabilizing proteins in lipid rafts [10]. On the other hand, clathrin-mediated internalization of specific anti-CAIX antibody VII/20, which binds to the CA domain is not disrupted by the loss of GAG structures, which can be critical during antibody-mediated drug delivery to CAIX-expressing hypoxic tumors. This different effect on CAIX-antibody complex internalization may be caused by the fact that the M75 antibody has a binding site in close proximity to the GAG glycan region, while the VII/20 antibody binds to the CAIX protein in the catalytic domain far away from the GAG attachment [45, 46].

Our article discusses yet unexplored roles of glycosylation in CAIX functions. As heparan sulfate and chondroitin sulfate proteoglycans are known to play an essential role in growth factor sequestration, we suppose that glycosaminoglycan structures in CAIX molecules containing HS/CS chains can also bind extracellular ligands, such as growth factors and cytokines, present them to their receptors and thereby stimulate downstream signaling pathways. This assumption is consistent with our results indicating the role of glycosaminoglycan structure in cell migration/invasion and EMT. As CAIX protein is localized on the plasma membrane and associated with tumors, it can be utilized as a promising therapeutic target. Our findings indicate that glycosylation of CAIX could be an integral part of the mechanisms by which cancer cells are able to adapt and respond to changing microenvironmental stimuli.

Supplementary information is available in the online version of the paper.

Acknowledgments: This work was supported by grants from the Slovak Scientific Grant Agency (VEGA 2/0095/23) and the Research & Developmental Support Agency (APVV-20-0480, APVV-20-0485, APVV-19-0098), and by the George Schwab and Leona Lauder Foundation. This publication was created thanks to support under the Operational Programme Integrated Infrastructure for the project: Strengthening of Research, Development and Innovation Capacities of Translational Biomedical Research of Human Diseases, IMTS: 313021BZC9, co-financed by the European Regional Development Fund.

References

- [1] HAUSELMANN I, BORSIG L. Altered Tumor-Cell Glycosylation Promotes Metastasis. *Front Oncol* 2014; 4: 1–15. <https://doi.org/10.3389/fonc.2014.00028>
- [2] ERNST B, MAGNANI JL. From Carbohydrate Leads to Glycomimetic Drugs. *Nat Rev Drug Discov* 2009; 8: 661–677. <https://doi.org/10.1038/nrd2852>
- [3] WEI J, HU M, HUANG K, LIN S, DU H. Roles of Proteoglycans and Glycosaminoglycans in Cancer Development and Progression. *Int J Mol Sci* 2020; 21: 1–28. <https://doi.org/10.3390/ijms21175983>
- [4] BROCKHAUSEN I, MELAMED J. Mucins as Anti-Cancer Targets: Perspectives of the Glycobiologist. *Glycoconj J* 2021; 38: 459–474. <https://doi.org/10.1007/s10719-021-09986-8>
- [5] HANSON RL, HOLLINGSWORTH MA. Functional Consequences of Differential O-Glycosylation of MUC1, MUC4, and MUC16 (Downstream Effects on Signaling). *Biomolecules* 2016; 6: 1–21. <https://doi.org/10.3390/biom6030034>
- [6] BHATIA R, GAUTAM SK, CANNON A, THOMPSON C, HALL BR et al. Cancer-Associated Mucins: Role in Immune Modulation and Metastasis. *Cancer Metastasis Rev* 2019; 38: 223–236. <https://doi.org/10.1007/s10555-018-09775-0>
- [7] WYKOFF CC, BEASLEY NJP, WATSON PH, TURNER KJ, PASTOREK J et al. Hypoxia-Inducible Expression of Tumor-Associated Carbonic Anhydrases 1. *Cancer Res* 2000; 60: 7075–7083.
- [8] PASTOREKOVA S, PARKKILA S, ZAVADA J. Tumor-Associated Carbonic Anhydrases and Their Clinical Significance. *Adv Clin Chem* 2006; 42: 167–216.
- [9] HILVO M, BARANAUSKIENE L, SALZANO AM, SCALONI A, MATULIS D et al. Biochemical Characterization of CAIX, One of the Most Active Carbonic Anhydrase Isozymes. *J Biol Chem* 2008; 283: 27799–27809. <https://doi.org/10.1074/jbc.M800938200>
- [10] CHRISTIANSON HC, MENARD JA, CHANDRAN VI, BOURSEAU-GUILMAIN E, SHEVELA D et al. Tumor Antigen Glycosaminoglycan Modification Regulates Antibody-Drug Conjugate Delivery and Cytotoxicity. *Oncotarget* 2017; 8: 66960–66974. <https://doi.org/10.18632/oncotarget.16921>
- [11] SVASTOVA E, HULIKOVA A, RAFAJOVA M, ZATOVICOVA M, GIBADULINOVA A et al. Hypoxia Activates the Capacity of Tumor-Associated Carbonic Anhydrase IX to Acidify Extracellular PH. *FEBS Lett* 2004; 577: 439–445. <https://doi.org/10.1016/j.febslet.2004.10.043>
- [12] SVASTOVA E, ZILKA N, ZATOVICOVA M, GIBADULINOVA A, CIAMPOR F et al. Carbonic anhydrase IX reduces E-cadherin-mediated adhesion of MDCK cells via interaction with β -catenin. *Exp Cell Res* 2003; 290: 332–345. [https://doi.org/10.1016/S0014-4827\(03\)00351-3](https://doi.org/10.1016/S0014-4827(03)00351-3)
- [13] SVASTOVA E, WITARSKI W, CSADEROVA L, KOSIK I, SKVARKOVA L et al. Carbonic Anhydrase IX Interacts with Bi-carbonate Transporters in Lamellipodia and Increases Cell Migration via Its Catalytic Domain. *J Biol Chem* 2012; 287: 3392–3402. <https://doi.org/10.1074/jbc.M111.286062>
- [14] CSADEROVA L, DEBREOVA M, RADVAK P, STANO M, VRESTIAKOVA M et al. The Effect of Carbonic Anhydrase IX on Focal Contacts during Cell Spreading and Migration. *Front Physiol* 2013; 4: 1–12. <https://doi.org/10.3389/fphys.2013.00271>
- [15] DEBREOVA M, CSADEROVA L, BURIKOVA M, LUKACIKOVA L, KAJANOVA I et al. CAIX Regulates Invasiveness Formation through Both a PH-Dependent Mechanism and Interplay with Actin Regulatory Proteins. *Int J Mol Sci* 2019; 20: 2745. <https://doi.org/10.3390/ijms20112745>
- [16] PASTOREKOVA S, ZAVADOVA Z, KOSTAL M, BABUSIKOVA O, ZAVADA J. A novel quasi-viral agent, MaTu, is a two-component system. *Virology* 1992;187(2):620–6. [https://doi.org/10.1016/0042-6822\(92\)90464-z](https://doi.org/10.1016/0042-6822(92)90464-z)
- [17] ZATOVICOVA M, TARABKOVA K, SVASTOVA E, GIBADULINOVA A, MUCHA V, JAKUBICKOVA L, et al. Monoclonal antibodies generated in carbonic anhydrase IX-deficient mice recognize different domains of tumour-associated hypoxia-induced carbonic anhydrase IX. *J Immunol Methods* 2003; 282(1–2):117–34. <https://doi.org/10.1016/j.jim.2003.08.011>
- [18] VIDLICKOVA I, DEQUIEDT F, JELENSKA L, SEDLAKOVA O, PASTOREK M et al. Apoptosis-Induced Ectodomain Shedding of Hypoxia-Regulated Carbonic Anhydrase IX from Tumor Cells: A Double-Edged Response to Chemotherapy. *BMC Cancer* 2016; 16: 239. <https://doi.org/10.1186/s12885-016-2267-4>
- [19] ZATOVICOVA M, SEDLAKOVA O, SVASTOVA E, OHRADANOVA A, CIAMPOR F et al. Ectodomain shedding of the hypoxia-induced carbonic anhydrase IX is a metalloprotease-dependent process regulated by TACE/ADAM17. *Brit J Cancer* 2005; 93: 1267–1276. <https://doi.org/10.1038/sj.bjc.6602861>
- [20] KAJANOVA I, ZATOVICOVA M, JELENSKA L, SEDLAKOVA O, BARATHOVA M et al. Impairment of carbonic anhydrase IX ectodomain cleavage reinforces tumorigenic and metastatic phenotype of cancer cells. *Brit J Cancer* 2020; 122: 1590–1603. <https://doi.org/10.1038/s41416-020-0804-z>
- [21] ZATOVICOVA M, PASTOREKOVA S. Modulation of Cell Surface Density of Carbonic Anhydrase IX by Shedding of the Ectodomain and Endocytosis. *Acta Virol* 2013; 57: 257–264. https://doi.org/10.4149/av_2013_02_257
- [22] LORENZEN I, LOKAU J, KORPYS Y, OLDEFEST M, FLYNN CM et al. Control of ADAM17 activity by regulation of its cellular localization. *Sci Rep* 2016; 6: 35067. <https://doi.org/10.1038/srep35067>
- [23] PEIXOTO A, RELVAS-SANTOS M, AZEVEDO R, LARA SANTOS L, FERREIRA JA. Protein Glycosylation and Tumor Microenvironment Alterations Driving Cancer Hallmarks. *Front Oncol* 2019; 9: 1–24. <https://doi.org/10.3389/fonc.2019.00380>
- [24] PASTOREK J, PASTOREKOVA S. Hypoxia-Induced Carbonic Anhydrase IX as a Target for Cancer Therapy: From Biology to Clinical Use. *Semin Cancer Biol* 2015; 31: 52–64. <https://doi.org/10.1016/j.semcancer.2014.08.002>

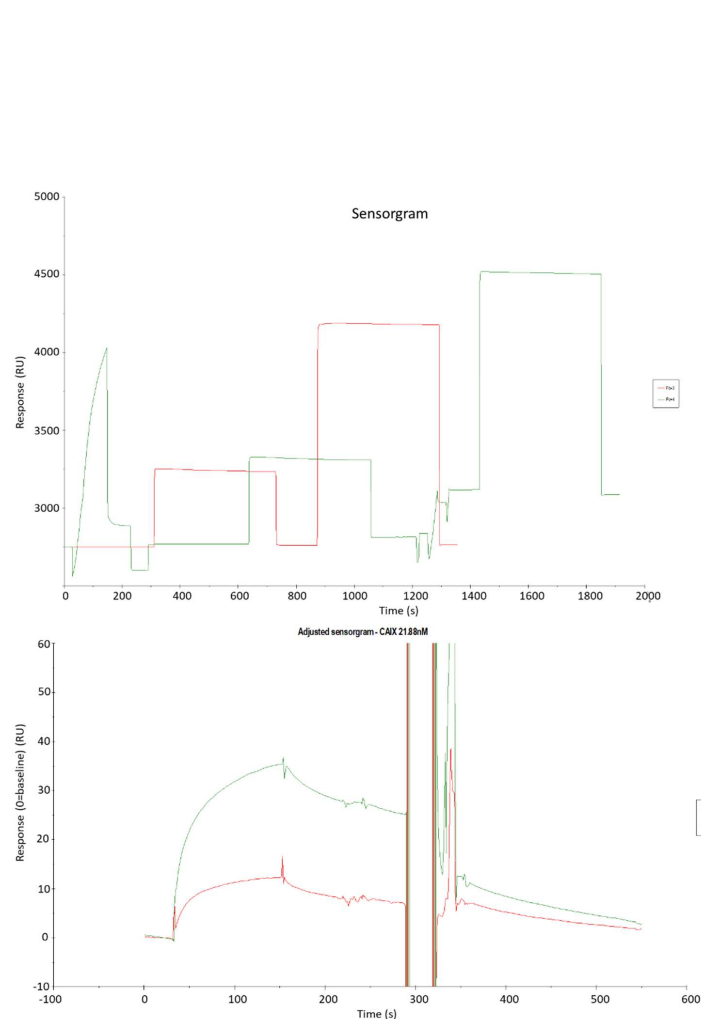
- [25] MERRY CLR, LINDAHL U, COUCHMAN J, ESKO JD. Proteoglycans and Sulfated Glycosaminoglycans. In: Varki A, Cummings RD, Esko JD, Stanley P, Hart GW, Aebi M, Mohren D, Kinoshita T, Packer NH, Prestegard JH, Schnaar RL, Seeberger PH (Eds.) *Essentials of Glycobiology* [Internet]. Cold Spring Harbor (NY): Cold Spring Harbor Laboratory Press, 2022. ISBN 978-1-621824-22-0
- [26] MIKAMI T, KITAGAWA H. Biosynthesis and Function of Chondroitin Sulfate. *Biochim Biophys Acta - Gen. Subj.* 2013; 1830: 4719–4733. <https://doi.org/10.1016/j.bbagen.2013.06.006>
- [27] IIDA J, PEI D, KANG T, SIMPSON MA, HERLYN M et al. Melanoma Chondroitin Sulfate Proteoglycan Regulates Matrix Metalloproteinase-Dependent Human Melanoma Invasion into Type I Collagen. *J Biol Chem* 2001; 276: 18786–18794. <https://doi.org/10.1074/jbc.M010053200>
- [28] IIDA J, WILHELMSON KL, NG J, LEE P, MORRISON C et al. Cell Surface Chondroitin Sulfate Glycosaminoglycan in Melanoma: Role in the Activation of pro-MMP-2 (pro-Matrilysin A). *Biochem J* 2007; 403: 553–563. <https://doi.org/10.1042/BJ20061176>
- [29] OLIVEIRA-FERRER L, LEGLER K, MILDE-LANGOSCH K. Role of Protein Glycosylation in Cancer Metastasis. *Semin Cancer Biol* 2017; 44: 141–152. <https://doi.org/10.1016/j.semcancer.2017.03.002>
- [30] ZATOVICOVA M, JELENSKA L, HULIKOVA A, CSADEROVA L, DITTE Z et al. Carbonic Anhydrase IX as an Anticancer Therapy Target: Preclinical Evaluation of Internalizing Monoclonal Antibody Directed to Catalytic Domain. *Curr Pharm Des* 2010; 16: 3255–3263. <https://doi.org/10.2174/138161210793429832>
- [31] KOKENYESI R. Ovarian Carcinoma Cells Synthesize Both CS and HS Cell Surface Proteoglycans That Mediate Cell Adhesion to Interstitial Matrix. *J Cell Biochem* 2001; 83: 259–270. <https://doi.org/10.1002/jcb.1230>
- [32] LIM CC, MULTHAUPT HAB, COUCHMAN JR. Cell Surface Heparan Sulfate Proteoglycans Control Adhesion and Invasion of Breast Carcinoma Cells. *Mol Cancer* 2015; 14: 1–18. <https://doi.org/10.1186/s12943-014-0279-8>
- [33] FUSTER MM, ESKO JD. The Sweet and Sour of Cancer: Glycans as Novel Therapeutic Targets. *Nat Rev Cancer* 2005; 5: 526–542. <https://doi.org/10.1038/nrc1649>
- [34] LAI J, CHIEN J, STAUB J, AVULA R, GREENE EL et al. Loss of HSulf-1 up-Regulates Heparin-Binding Growth Factor Signaling in Cancer. *J Biol Chem* 2003; 278: 23107–23117. <https://doi.org/10.1074/jbc.M302203200>
- [35] THAKUR N, GUDEY SK, MARCUSSON A, FU JY, BERGH A et al. TGF β -induced invasion of prostate cancer cells is promoted by c-Jun-dependent transcriptional activation of Snail1. *Cell Cycle* 2014; 13: 2400–2414. <https://doi.org/10.4161/cc.29339>
- [36] AN J, LIU H, MAGYAR CE, GUO Y, VEENA MS et al. Hyperactivated JNK is a therapeutic target in pVHL-deficient renal cell carcinoma. *Cancer Res* 2013; 73: 1374–1385. <https://doi.org/10.1158/0008-5472.CAN-12-2362>
- [37] OHKUBO T, OZAWA M. The transcription factor Snail downregulates the tight junction components independently of E-cadherin downregulation. *Cell Sci* 2003; 117: 1675–1685. <https://doi.org/10.1242/jcs.01004>
- [38] LEE TK, POON RTP, YUEN AP, LING MT, KWOK WK et al. Twist overexpression correlates with hepatocellular carcinoma metastasis through induction of epithelial-mesenchymal transition. *Clin Cancer Res* 2006; 12: 5369–5376. <https://doi.org/10.1158/0008-5472.CAN-12-2362>
- [39] SWAYAMPAKULA M, MCDONALD PC, VALLEJO M, COYAUD E, CHAFE SC et al. The Interactome of Metabolic Enzyme Carbonic Anhydrase IX Reveals Novel Roles in Tumor Cell Migration and Invadopodia/MMP14-Mediated Invasion. *Oncogene* 2017; 36: 6244–6261. <https://doi.org/10.1038/onc.2017.219>
- [40] BARAZI HO, ZHOU L, TEMPLETON NS, KRUTZSCH HC, ROBERTS DD. Identification of heat shock protein 60 as a molecular mediator of $\alpha\beta 1$ integrin activation. *Cancer Res* 2002; 62: 1541–1548.
- [41] WU YM, NOWACK DD, OMENN GS, HAAB BB. Mucin glycosylation is altered by pro-inflammatory signaling in pancreatic-cancer cells. *J Proteome Res* 2009; 8: 1876–1886. <https://doi.org/10.1021/pr8008379>
- [42] GHOSH SK, PANTAZAPOULOS P, MEDAROVA Z, MOORE A. Expression of underglycosylated MUC1 antigen in cancerous and adjacent normal breast tissues. *Clin Breast Cancer* 2013; 13: 109–118. <https://doi.org/10.1016/j.clbc.2012.09.016>
- [43] SINGH R, BANDYOPADHYAY D. MUC1: a target molecule for cancer therapy. *Cancer Biol Ther* 2007; 64: 481–486. <https://doi.org/10.4161/cbt.6.4.4201>
- [44] KAUR S, KUMAR, S, MOMI N, SASSON AR, BATRA SK. Mucins in pancreatic cancer and its microenvironment. *Nature Rev Gastroenterol Hepatol* 2013; 10: 607–620. <https://doi.org/10.1038/nrgastro.2013.120>
- [45] ZAVADA J, ZAVADOVA Z, PASTOREK J, BIESOVA Z, JEZEK J et al. Human tumour-associated cell adhesion protein MN/CA IX: identification of M75 epitope and of the region mediating cell adhesion. *Brit J Cancer* 2000; 82: 1808–1813. <https://doi.org/10.1054/bjoc.2000.1111>
- [46] ZATOVICOVA M, TARABKOVA K, SVASTOVA E, GIBADULINOVA A, MUCHA V et al. Monoclonal antibodies generated in carbonic anhydrase IX-deficient domains of tumour-associated hypoxia-induced carbonic anhydrase IX. *J Immunol Methods* 2003; 282: 117–134. <https://doi.org/10.1016/j.jim.2003.08.011>
- [47] BIZIK J, KANKURI E, RISTIMAKI A, TAIEB A, VAPAAT-ALO H et al. Cell-cell contacts trigger programmed necrosis and induce cyclooxygenase-2 expression. *Cell Death Differ* 2004; 11: 183–195. <https://doi.org/10.1038/sj.cdd.4401317>

https://doi.org/10.4149/neo_2023_230505N246

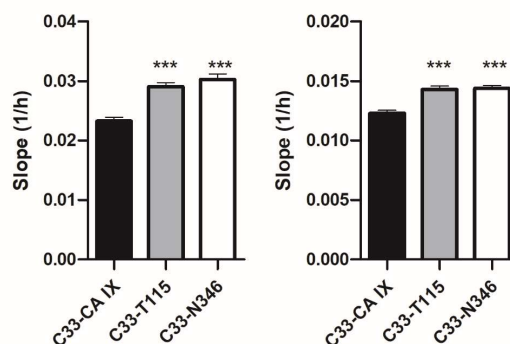
Functional consequences of altered glycosylation of tumor-associated hypoxia biomarker carbonic anhydrase IX

Magdalena BARATOVA*, Lucia SKVARKOVA*, Maria BARTOSOVA, Lenka JELENSKA, Miriam ZATOVICOVA, Barbora PUZDEROVA, Ivana KAJANOVA, Lucia CSADEROVA*, Silvia PASTOREKOVA, Eliska SVASTOVA

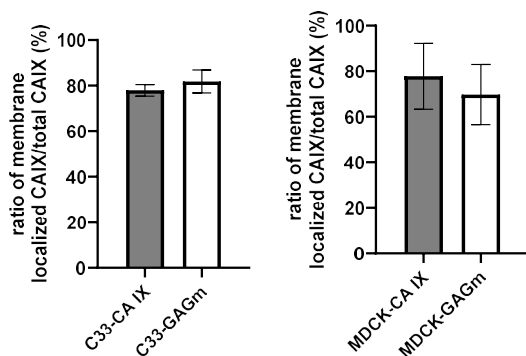
Supplementary Information



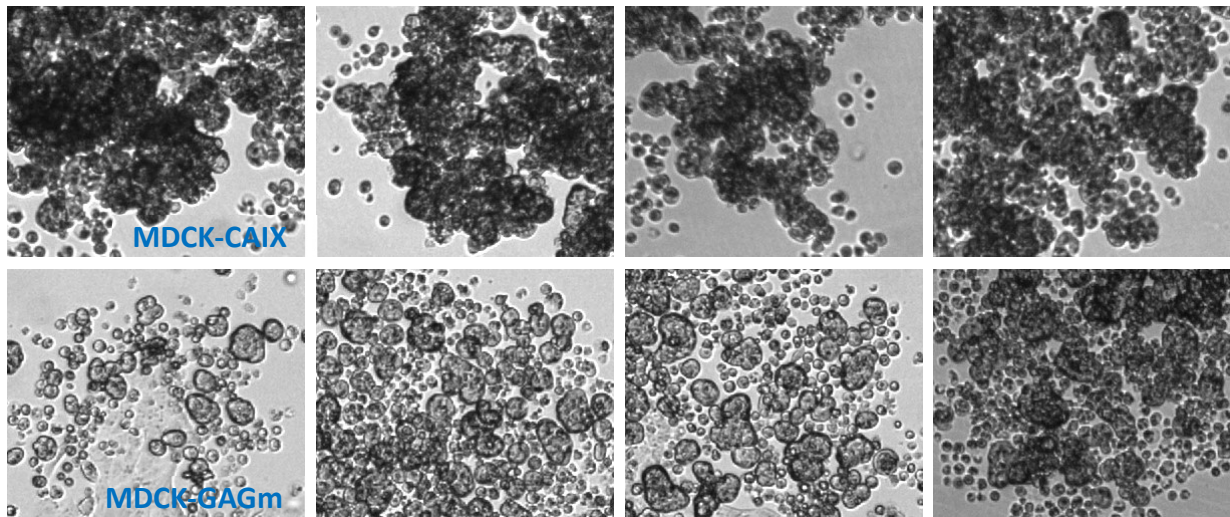
Supplementary Figure S2. Protein-protein interaction analysis with the BIAcore 2000 system. Collagen was immobilized on CM5 sensor chip under acidic conditions (upper panel). Interaction analysis of CAIX-SBP to collagen after regeneration with 4M MgCl₂ (lower panel).



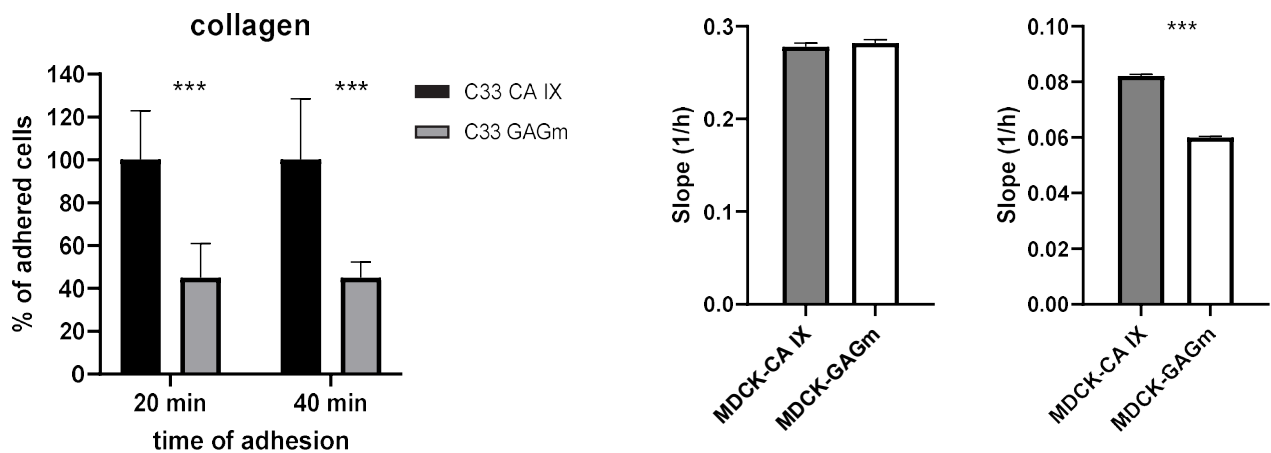
Supplementary Figure S1. Transwell migration (left) and invasion assay (right) performed at xCELLigence system with C33 cells expressing wild type, N346, and T115-mutated CAIX. Representative graphs give mean \pm SD of the slopes, measured in quadruplicates, reflecting the migration/invasion rate of the cells during chemotactic assay. The significance of differences was assessed by one-way ANOVA with Dunnett's multiple comparison post-hoc test, denotes *** p <0.001.



Supplementary Figure S3. ELISA comparing membrane-bound amount of CAIX in live cells and the total amount of CAIX in fixed cells. The graph gives mean \pm SD of membrane/total CAIX ratio measured in three independent experiments in pentaplicates. Possible differences were evaluated by Student's t-test and found non-significant.



Supplementary Figure S4. Representative images of cell aggregates. MDCK-GAGm cells (lower panel) exhibited diminished cell-cell contacts and formation of smaller aggregates in comparison to MDCK-CAIX cells (upper panel). Images were acquired at Zeiss Axiovert 40 CFL, 10× objective.

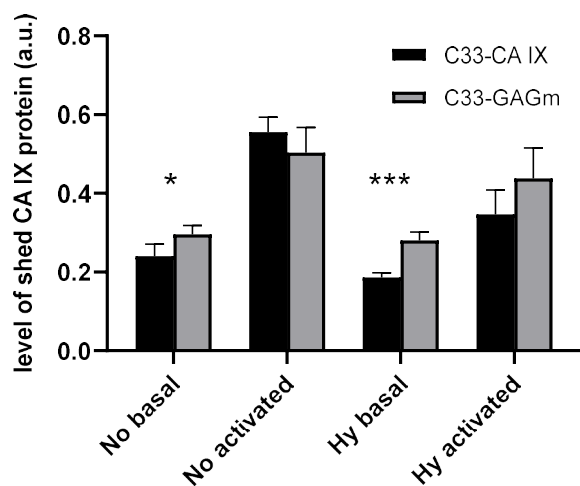


Supplementary Figure S5. Adhesion of C33 cells expressing wild type and CAIX-GAGm to collagen. Cell adhesion is expressed as percentage of adhered cells when compared to C33 CAIX (set as 100%). Values are expressed as mean±SD, significance of differences was evaluated by Student's t-test in comparison to control C33-CAIX cells, ***p<0.001.

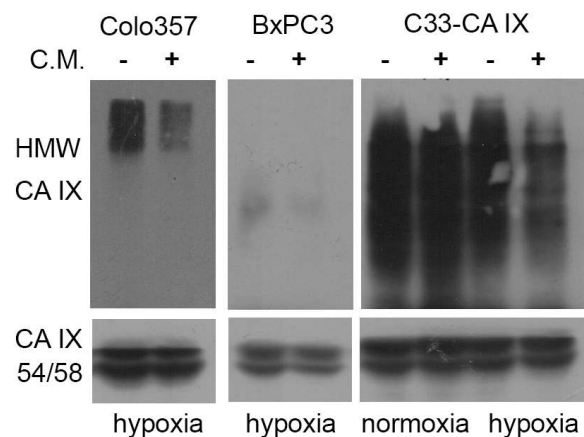
Supplementary Figure S6. Transwell migration (left) and invasion assay (right) performed at xCELLigence system with MDCK cells expressing wild type and CAIX-GAGm. Slopes illustrate the migration rate of the cells. Values are expressed as mean±SD, significance of differences was evaluated by Student's t-test in comparison to control C33-CAIX cells, ***p<0.001.

Supplementary Table S1. List of the primers used for RT-PCR analysis of the gene expression associated with epithelial-mesenchymal transition.

mRNA	sense primer	antisense primer
Snail1	5'-caactgcaactactgcaacaagga-3'	5'-acttctgacatctgagtggtctg-3'
Twist1	5'-catcctcacacctctgattct-3'	5'-actatggtttgcaggccagt-3'
MMP14	5'-gcaattcgtcttctctcaagg-3'	5'-tgttctggggtactcgtatc-3'
VEGFA	5'-cttgctctctacctccacct-3'	5'-cacacagatggctgaagatg-3'
Slug	5'-tgatgaagaggaaagactacartcc-3'	5'-cttctcccmtgtgagttctaat-3'
Fibronectin	5'-ttacagttcaggttctctgg-3'	5'-cccacttctccaactctg-3'
β-actin	5'-tctccctggagaagagcta-3'	5'-acatctgctggaaggtggac-3'

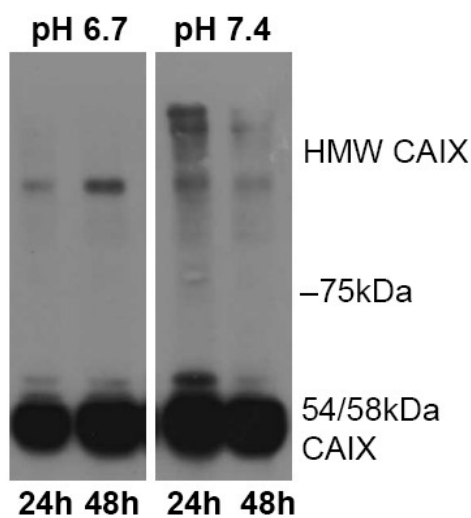


Supplementary Figure S7. Shedding of CAIX ectodomain in the culture media of C33-CAIX and GAGm cells determined by ELISA. Data were normalized on total protein concentration and concentration of CAIX. All data represent means±SD, *p<0.05, **p<0.01, ***p<0.001 in comparison to control C33-CAIX cells under the same conditions evaluated by Student's t-test.



Supplementary Figure S8. Impact of inflammatory environment on GAG glycosylation of CAIX. Western blot analysis of CAIX in pancreatic cell lines BxPC3 and Colo357 and C33-CAIX transfectants cultured in inflammatory medium from MUF fibroblasts (+C.M.) and in control DMEM medium (-C.M.). Inflammatory media reduced the amount of GAGs on CAIX protein in hypoxic pancreatic cancer cells BxPC3 (reduction by 15%) and COLO357 (by 45%) compared to their cultivation in DMEM media. Importantly, C33 cells with ectopic CAIX expression show reduced GAG structures on CAIX under hypoxic (reduction by 50%) but not in normoxic conditions.

Human dermal fibroblasts (MUF) were kindly provided by Dr. Jozef Bizik, and inflammatory conditioned media were prepared according to the protocol published in Bizik et al. 2004 [47]. BxPC3, COLO357, and C33 CAIX cells were seeded in DMEM media (600,000 cells/3.5 cm Petri dish), and 24 h after seeding in selected samples control media was exchanged for inflammatory media for 32 h.



Supplementary Figure S9. Western blot analysis of 54/58 kDa form and HMW form CAIX in control fibrosarcoma HT1080 cells (routinely cultured under pH 7.4) and HT1080 cells adapted to low pH of 6.7 cultured in hypoxia for 24 h and 48 h. The blot shows reduced amount of GAG modification in cells cultured under low pH conditions.